

# Optimising Surfactant Aided Dispersions of Carbon Nanotubes in Aqueous Solution

A.J. Blanch, C.E. Lenehan, and J.S. Quinton

School of Chemical and Physical Sciences,  
Flinders University, GPO Box 2100,  
Adelaide, SA 5001, Australia

**Abstract** – Dispersion of carbon nanotubes in water with the aid of surfactants is becoming common practice, however methodologies vary greatly among the literature. Here the variables of sonication type, length of processing time and power input are examined to find optimal values for dispersion of arc-discharge nanotubes in sodium dodecylbenzene sulfonate.

**Keywords** - Carbon Nanotube, Surfactant, Dispersion, Raman, UV-Vis Spectroscopy

## I. INTRODUCTION

Carbon Nanotubes (CNTs) have long been recognised as a promising material for a variety of applications due to their remarkable properties. However, their implementation has been hampered by the intractability of as produced CNT soot, where the CNTs adhere to each other strongly in ropes or bundles through van der Waals forces [1]. This is usually coupled with a broad diameter and length distribution within the nanotubes, while a high level of impurities such as non-nanotube carbonaceous material and residual metal catalyst particles from the synthesis process are often present [2; 3]. Many methods exist to purify and/or disperse raw carbon material, with aims towards removing the metal catalyst and amorphous carbon, and further toward separation by length, diameter or electronic type. The majority of such separation techniques require the nanotubes to be individualised, and this is usually achieved through ultrasonic exfoliation of the bundles in an organic solvent or an aqueous solution containing some dispersive agent, such as a surfactant, polymer, oligonucleotide or DNA, among others [4]. Often a consecutive ultracentrifugation step is employed to remove remaining larger bundles, to leave primarily individual nanotubes and small bundles in the supernatant. Centrifugation has the added advantage of purifying the CNT soot by removing the heavier metal catalyst particles and larger carbonaceous/non-nanotube material from the solution [2].

Since so many variables exist for these dispersions (nanotube/surfactant types and concentrations, sonication type, power and time, ultracentrifugation speed and time etc.) it is unsurprising that dispersion parameters vary significantly in the literature. For this reason, a parametric study of a selection of these variables has been performed in order to better understand the dispersion processes and therefore find optimal values for the materials used.

## II. EXPERIMENTAL

Surfactant dodecylbenzene sulfonate (SDBS) and sodium dodecyl sulfate (SDS) were purchased from Sigma-Aldrich and used as received. These surfactants are commonly used for CNT dispersion and have been shown to be effective at concentrations ~1wt% [5]. As produced electric arc (Carbon Solutions) CNTs were dispersed in 14.3mM (0.5wt%) aqueous SDBS solutions via bath (Elmasonic S30H, 37kHz) or tip (Sonics VCX 750W, 20kHz with 5 or 6.5mm Ti microtip) ultrasonication. In both instances the samples were cooled with ice water. Samples were ultracentrifuged at fixed angle immediately after sonication (Beckman-Coulter Optima L-100XP, Type 50 Ti rotor) and the upper ~70-85% of the supernatant was collected via pipette. UV-Vis-NIR spectra were recorded on a Cary 5G spectrophotometer at 600nm/min using quartz cuvettes with surfactant solution backgrounds subtracted. Raman spectra of 200 $\mu$ l aliquots of each sample were acquired on a WiTEC confocal Raman  $\alpha$ -300 spectrometer utilising a 532nm laser coupled to a Nikon 40x objective, with the focal plane aligned ~15-20 $\mu$ m below the solution surface. Multiple accumulations of 1-60 seconds each were collected for all samples, and manual baseline subtraction was performed with Fityk analysis software.

## III. RESULTS AND DISCUSSION

A typical UV-Vis-NIR spectrum of arc nanotubes dispersed in water with SDBS is shown in Fig. 1. CNTs

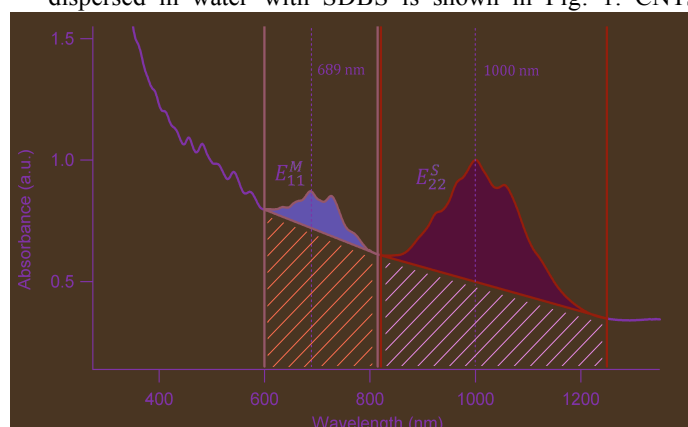


Figure 1: UV-Vis-NIR spectrum of arc nanotubes dispersed in 14.3mM SDBS via tip sonication (10min, 20%) and centrifuged at ~122000xg for 1 hour. Peak areas are obtained by subtraction of a linear baseline, with the 'resonance ratio' calculated using the nanotube peak area (solid) over the non-resonant background (shaded).

exhibit absorbance peaks arising from transitions between van Hove singularities in the valence and conductive bands of the nanotube's electronic density of states, and these absorptions have also been shown to be excitonic in nature [6]. These convoluted peaks can be grouped according to their corresponding transition  $E_{ii}^{S,M}$ , where  $i$  is the order of the transition from  $c_i$  to  $v_i$ , and M and S denote transitions for 'metallic' and 'semiconducting' tubes respectively. Well dispersed nanotube solutions exhibit larger peaks due to nanotube absorptions, with peaks from individual species becoming more resolved as the nanotubes are further exfoliated. Broader, red shifted peaks are obtained for more bundled suspensions [7]. For UV-Vis-NIR trends the peak areas of the  $E_{22}^S$  (S22) and  $E_{11}^M$  (M11) peak groups centered at  $\sim 1000\text{nm}$  and  $\sim 689\text{nm}$  respectively were used as indicators of the relative amount of nanotubes dispersed, while the 'resonance ratio' (the ratio of the nanotube peaks to the non-resonant background of the carbon  $\pi$ -plasmon and other contributions) was used to reflect the 'purity' state of the solution [3]. A larger such ratio may suggest a greater proportion of nanotubes suspended compared to non-nanotube material, or a less damaged sample; the background signal is expected to increase as nanotubes are fragmented. Both S22 and M11 peaks were analysed, however since the CNT raw product contains approximately 2/3 semiconducting and 1/3 metallic nanotubes, only the semiconducting nanotube peaks are presented here. It should be noted that both peak groups scale proportionally along the same trend for all dispersion analyses.

Fig.2A shows the evolution of the S22 absorbance peak of arc CNTs in SDS over time. The loss of fine structure implies that the CNTs are gradually re-aggregating. It has previously been noted that SDS disperses smaller HiPCO type nanotubes well, having diameters from  $\sim 0.7\text{-}1.1\text{nm}$ , but is a poor surfactant for larger diameter nanotubes [1]. Arc type tubes have a relatively narrow diameter distribution from around  $1.3\text{-}1.5\text{nm}$ , at the larger end of the single-walled CNT diameter spectrum, hence SDS is not very suitable. Fig. 2B shows the evolution of the S22 peak area and resonance ratio, both parameters following a similar decreasing trend to the absorbance itself. Both are sensitive to the re-aggregation of the nanotubes, and hence peak area and resonance ratio may tentatively be used as relative measures of dispersion quality. SDBS performs much better than SDS for arc type nanotubes, with the absorbance spectrum being more resolved and stable for many months after production, though some visible re-bundling does eventually occur.

A Raman spectrum of arc nanotubes dispersed in SDBS is shown in Fig. 2C, displaying the characteristic nanotube peaks; the radial breathing mode (RBM) arising from expansion and contraction of the nanotube about its central axis ( $\sim 167\text{cm}^{-1}$  in this case), the disorder induced mode D ( $\sim 1337\text{cm}^{-1}$ ), the G band arising from vibrations along the axis and around the circumference of the tube ( $\sim 1586\text{cm}^{-1}$ ), the M band which is an overtone of an out-of-plane mode from graphite ( $\sim 1745\text{cm}^{-1}$ ), and the G' band which is a second harmonic of the D band, but is less sensitive to defects ( $\sim 2768\text{cm}^{-1}$ ) [8]. The broad peak from  $3000\text{-}3700\text{cm}^{-1}$  is attributed to stretching modes of OH groups in water. For

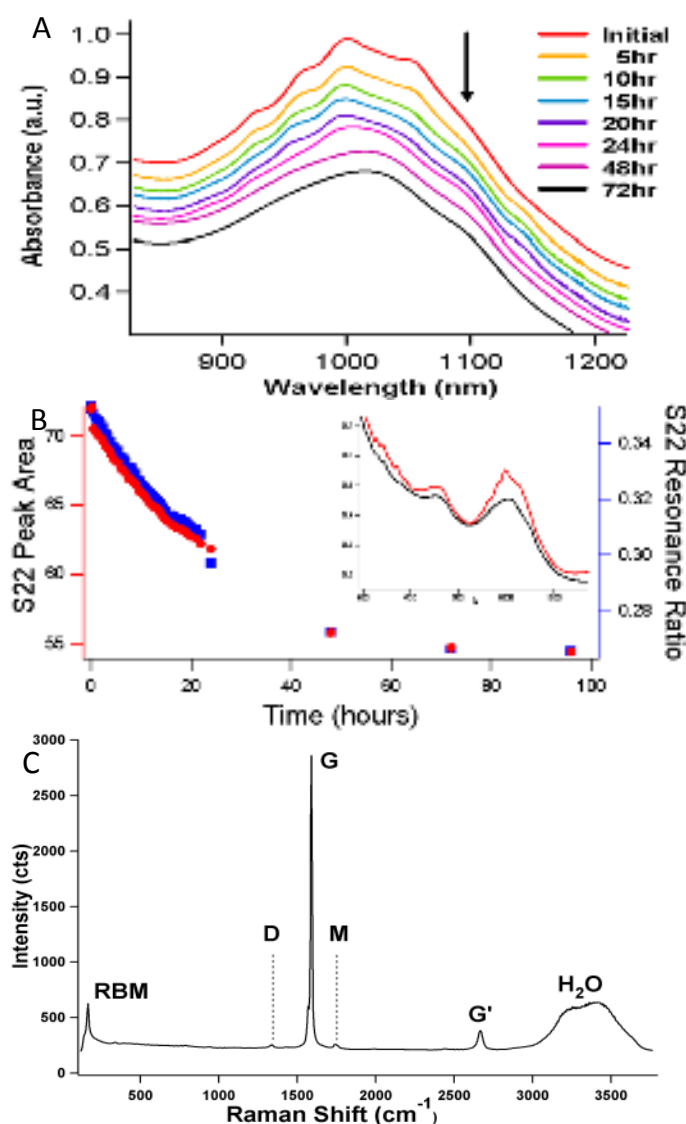


Figure 2: (A) UV-Vis spectra of the S22 region of arc CNTs dispersed in 34.7mM SDS, showing loss of fine structure over time. Spectra are offset for clarity. (B) Evolution of the S22 peak area (red) and S22 resonance ratio (blue) over time as the nanotubes re-aggregate. Inset: broader spectrum view of CNTs in SDS, immediately after dispersion (red) and 2 months later (black). (C) Raman spectrum of arc nanotubes dispersed in 14.3mM SDBS via tip sonication, displaying the characteristic Raman bands for single-walled CNTs.

Raman analysis of the samples the intensity of the bands was used as an indicator of the amount of nanotubes dispersed in solution, and it was observed that these followed approximately the same trend as the UV-Vis-NIR peak areas. The Raman D:G ratio was also measured as it is considered to be associated with the purity of the solution in some form, as the D-band is related to defects in the CNT structure as well as the amorphous carbon content [8]. Thus a lower D:G ratio suggests a more pure CNT sample, or one with fewer overall defects.

To examine the effect of sonication time on the resultant dispersions, a series of samples of  $0.5\text{mg/mL}$  raw arc CNT in  $14.3\text{mM}$  SDBS were prepared and subjected to three different methods of ultrasonication (Fig. 3). For bath

sonication, the amount of nanotubes in the supernatant continues to increase with time up to about 5 hours, while saturation is realised at about 30 minutes for the 5mm tip, and after ~2.5hrs for the 6.5mm tip. Tip sonicated samples have a greater amount of nanotubes remaining in the supernatant after short processing times, as tip sonication is far more efficient with a more intense energy input. The two microtips were driven at 20% amplitude, delivering an approximate power of 10 and 8W to the solution respectively. For the 5mm tip repeat sets of individual 10mL samples were run and as such each point is an average of 2-3 samples. For both the 6.5mm tip and bath sonication series a large volume of solution was made and aliquots of 10mL were removed after the allocated times. This difference in sampling method may account for a portion of the observed difference in the rate of increase in CNT concentration with time between the two probe tips. Fig. 3D compares these two series in terms of power delivered per volume of solution, showing a similar dispersion performance. Indeed, if anything, the larger diameter tip performs better per unit volume. It is evident that the volume of solution being dispersed, and likely the geometry of the sample vessel involved, influences the overall energy density imparted to the system and hence the CNT concentration of the resultant dispersion.

Both the resonance ratio (Fig. 3B) and Raman D:G ratio (Fig. 3C) suggest that the more rapid increase in nanotube concentration from tip sonication is coupled to an increase in damage caused to the nanotubes, probably through tube scission and sidewall defect generation. The RBM:G and G':G ratios are observed to remain essentially constant for each sample set (not shown). While the D:G ratio continues to increase with processing time for both tip sets, the bath sonication samples appear to produce a minimum at about 1 hour, corresponding also to the inflection in the S22 resonance ratio. The turning point in the resonance ratio corresponds to a greater increase in the background absorbance compared to that of the CNTs, which may indicate an increase in damage to the sample; i.e. after a certain sonication time more defects are produced than nanotubes are being exfoliated, thus intermediate times may offer a compromise between the obtained CNT concentration and nanotube integrity. It is apparent that the optimal sonication time will depend on the specifics of the system under observation, as the choice of sonication type, tip size, solution volume as well as the nanotube and surfactant types all have an influence.

Samples of raw arc CNT in SDBS were prepared and ultrasonicated at different sonication tip amplitudes using the 5mm tip, followed by centrifugation under the same conditions used previously. A sonication time of 10 minutes was used to allow high throughput, as well as to minimise damage to the CNTs. Fig. 4A shows that as the amplitude (and thus the energy delivered to the system) is increased from 20 to 30%, the amount of nanotubes remaining in the supernatant decreases rapidly, while an amplitude above 30% yields approximately the same level of absorbance. This change in yield is linked closely with the onset of foam formation at higher power. The formation of surfactant

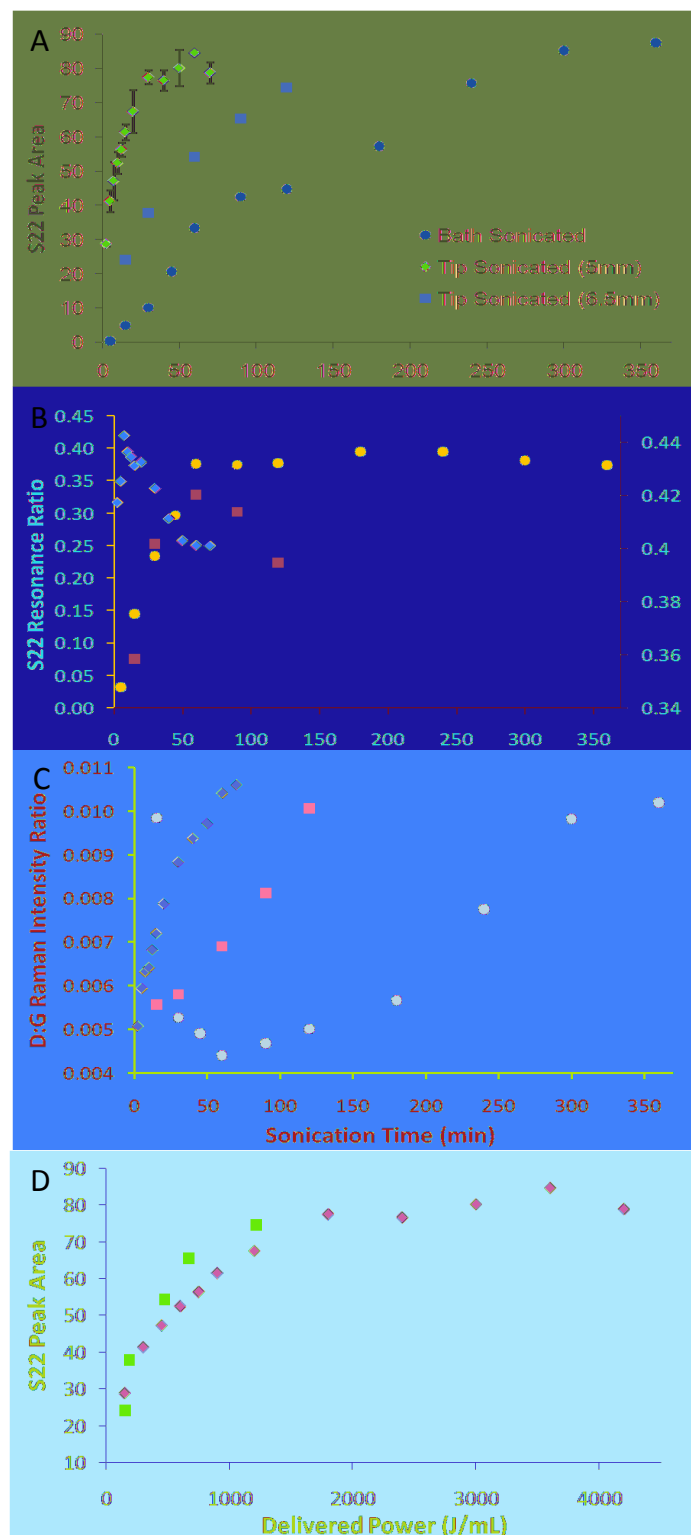


Figure 3: UV-Vis-NIR peak areas (A), and resonance ratios (B) for the S22 nanotube peak, with Raman D:G intensity ratios (C) as a function of sonication time for both 5 and 6.5mm tip sonication (blue, green) and bath sonication (red). A comparison of the two microtips in terms of power delivered per mL to the sample is given in (D). Samples were suspended in 14.3mM SDBS, with the tip sonicator driven at 20% amplitude. Series were centrifuged at 122000xg for 1 hour. Note: in (B) the left axis is bath sonicated samples, while both tip sets are plotted on the right.

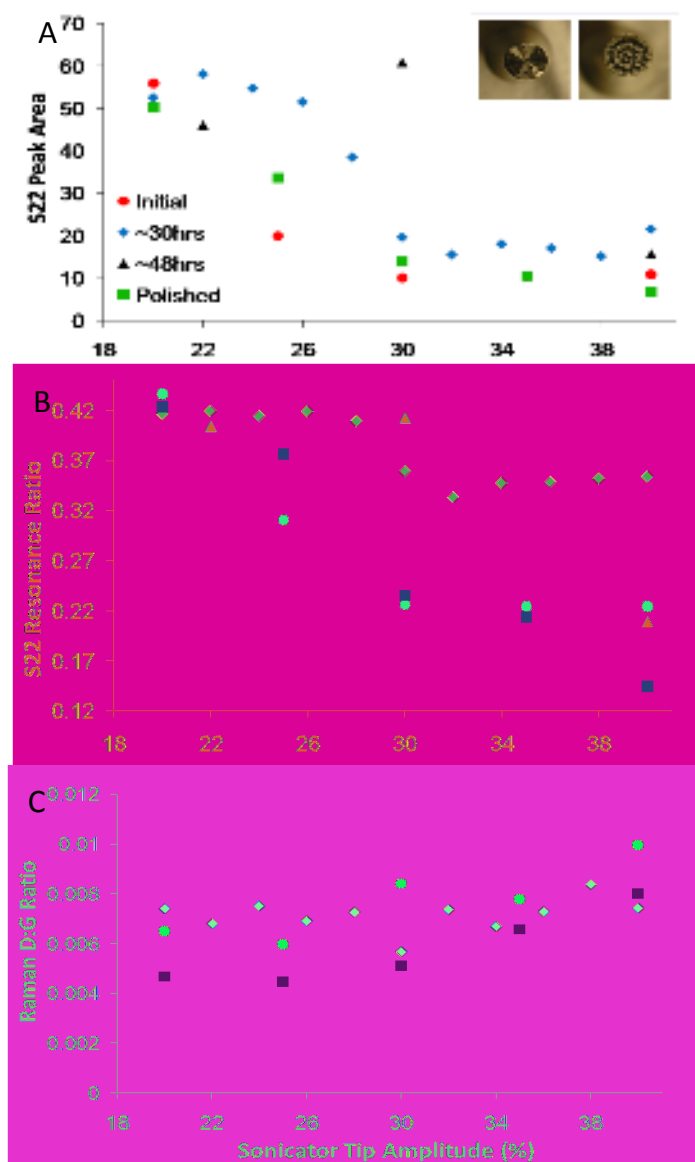


Figure 4: UV-Vis-NIR peak areas (A) and resonance ratios (B) for the S22 nanotube peak with Raman D:G intensity ratios (C) as a function of sonication amplitude (power) for the 5mm microtip. From the initial state (red), the condition of the tip deteriorates after 30 (blue) and 48 (black) cumulative hours of operation, with restoration of performance after polishing of the tip (green). Inset: the sonicator tip showing a initial stages of pitting (left) and excessive pitting after 48 hours of operation (right).

foams is known to impede dispersion, perhaps as the free surfactant is held in the interface of bubble walls and is therefore unable to adsorb on a nanotube sidewall. It seems that low power sonication is more suitable for generating CNT dispersions; however one method to increase CNT concentration with higher intensity sonication may be the addition of a suitable antifoam agent, or to use a dispersant that does not form a stable foam [9]. Still, sonication at higher power may lead to greater damage inflicted upon the nanotubes, as suggested here by the increase and decrease in Raman D:G and S22 resonance ratios respectively.

Under normal operation, the sonicator tip gradually degrades, with pits forming on the originally flat surface. As a result, small amounts of Ti are also added to the dispersion as the tip is eroded, though these are removed in the centrifugation step. In Fig.4A it is apparent that over time the tip loses conversion efficiency, and the power delivered to the sample slowly decreases as the surface of the tip becomes more pitted. This is observed in the shift of the curve, with gradually greater amounts of CNTs dispersed at the intermediate tip amplitudes, and less dispersed at lower power. Using a lathe to polish the tip back to a flat surface results in recovery of close to the original trend, despite changing the length of the resonant tip.

#### IV. CONCLUSION

The production of CNT suspensions is dependent on many variables, and the parameters for a 'good' dispersion cannot be strictly defined. This study would suggest that tip ultrasonication is more effective than bath sonication, and longer sonication times will exfoliate more nanotubes from larger bundles although the extent of ultrasound induced damage to the nanotubes likely increases also. Foam formation during sonication is found to correspond to large decrease in dispersion. Lower powers are recommended as significantly more nanotubes are suspended in the supernatant, and less damage is caused to the CNTs.

#### ACKNOWLEDGEMENT

A.B. would like to thank Dr. Milena Ginic-Markovic for use of the Sonics VCX 750W.

#### REFERENCES

- [1] T.J. McDonald, C. Engrakul, M. Jones, G. Rumbles, and M.J. Heben, "Kinetics of PL quenching during single-walled carbon nanotube rebundling and diameter-dependent surfactant interactions". *J. Phys. Chem. B*, vol. 110, pp. 25339-25346, 2006.
- [2] D. Nishide, Y. Miyata, K. Yanagi, T. Tanaka, and H. Kataura, "PERIPUTOS: Purity evaluated by Raman intensity of pristine and ultracentrifuged topping of single-wall carbon nanotubes". *physica status solidi (b)*, vol. 246, pp. 2728-2731, 2009.
- [3] M.E. Itkis, D.E. Perea, R. Jung, S. Niyogi, and R.C. Haddon, "Comparison of analytical techniques for purity evaluation of single-walled carbon nanotubes". *J. Am. Chem. Soc.*, vol. 127, pp. 3439-3448, 2005.
- [4] H. Wang, "Dispersing carbon nanotubes using surfactants". *Current Opinion in Colloid & Interface Science*, vol. 14, pp. 364-371, 2009.
- [5] V.C. Moore, et al., "Individually suspended single-walled carbon nanotubes in various surfactants". *Nano Lett.*, vol. 3, pp. 1379-1382, 2003.
- [6] P. Avouris, M. Freitag, and V. Perebeinos, "Carbon-nanotube photonics and optoelectronics". *Nat Photon*, vol. 2, pp. 341-350, 2008.
- [7] M.J. O'Connell, et al., "Band gap fluorescence from individual single-walled carbon nanotubes". *Science*, vol. 297, pp. 593-596, 2002.
- [8] M.S. Dresselhaus, G. Dresselhaus, R. Saito, and A. Jorio, "Raman spectroscopy of carbon nanotubes". *Physics Reports*, vol. 409, pp. 47-99, 2005.
- [9] H. Sato, and M. Sano, "Characteristics of ultrasonic dispersion of carbon nanotubes aided by antifoam". *Colloids and Surfaces A: Physicochemical and Engineering Aspects*, vol. 322, pp. 103-107, 2008.